

# Conformational Properties of 1-Silyl-1-Silacyclohexane, C<sub>5</sub>H<sub>10</sub>SiHSiH<sub>3</sub>: Gas Electron Diffraction, Low-Temperature NMR, Temperature-Dependent Raman Spectroscopy, and Quantum Chemical Calculations<sup>&</sup>

Sunna Ó. Wallevik,<sup>†,‡</sup> Ragnar Bjornsson,<sup>†,‡</sup> Ágúst Kvaran,<sup>†</sup> Sigridur Jonsdottir,<sup>†</sup> Ingvar Arnason,<sup>\*,†</sup> Alexander V. Belyakov,<sup>§</sup> Alexander A. Baskakov,<sup>§</sup> Karl Hassler,<sup>||</sup> and Heinz Oberhammer<sup>⊥</sup>

Science Institute, University of Iceland, Dunhaga 3, IS-107 Reykjavik, Iceland, School of Chemistry, North Haugh, University of St Andrews, St Andrews, Fife, KY16 9ST, U.K., Saint-Petersburgh State Technological Institute, Saint-Petersburgh 190030, Russia, Technische Universität Graz, Stremayergasse 16, A-8010 Graz, Austria, and Institut für Physikalische und Theoretische Chemie, Universität Tübingen, 72076 Tübingen, Germany

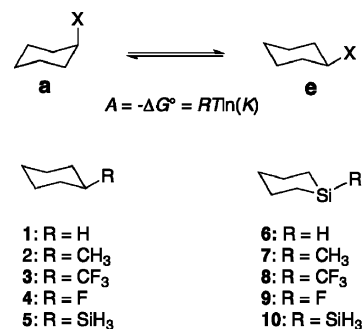
Received: October 16, 2009; Revised Manuscript Received: December 18, 2009

The molecular structure of axial and equatorial conformers of 1-silyl-silacyclohexane, C<sub>5</sub>H<sub>10</sub>SiHSiH<sub>3</sub>, and the thermodynamic equilibrium between these species were investigated by means of gas electron diffraction (GED), dynamic nuclear magnetic resonance (DNMR), temperature-dependent Raman spectroscopy, and quantum chemical calculations (CCSD(T), MP2 and DFT methods). According to GED, the compound exists as a mixture of two conformers possessing the chair conformation of the six-membered ring and C<sub>s</sub> symmetry and differing in the axial or equatorial position of the SiH<sub>3</sub> group (axial = 57(7) mol %/equatorial = 43(7) mol %) at T = 321 K. This corresponds to an A value (free energy difference = G<sub>axial</sub> – G<sub>equatorial</sub>) of –0.17(15) kcal mol<sup>–1</sup>. A low-temperature <sup>13</sup>C NMR experiment using SiD<sub>4</sub> as a solvent resulted in an axial/equatorial ratio of 45(3)/55(3) mol % at 110 K corresponding to an A value of 0.05(3) kcal mol<sup>–1</sup>, and a ΔG<sup>#</sup> value of 5.7(2) kcal mol<sup>–1</sup> was found at 124 K. Temperature-dependent Raman spectroscopy in the temperature range of 210–300 K of the neat liquid, a THF solution, and a heptane solution indicates that the axial conformer is favored over the equatorial one by 0.26(10), 0.23(10), and 0.22(10) kcal mol<sup>–1</sup> (ΔH values), respectively. CCSD(T)/CBS and MP2/CBS calculations in general predict both conformations to have very similar stability and are, thus, in excellent agreement with the DNMR result but in a slight disagreement with the GED and Raman results. Two DFT functionals, that account for dispersion interactions, M06-2X/pc-3 and B2PLYP-D/QZVPP, deviate from the high-level coupled cluster and MP2 calculations by only 0.1 kcal mol<sup>–1</sup> on average, whereas B3LYP/pc-3 calculations greatly overestimate the stability of the equatorial conformer.

## Introduction

The conformational behavior of six-membered ring systems, steric effects of substituents, and stereoelectronic interactions in the ring systems continue to be an active field of research.<sup>2–8</sup> Cyclohexane and its derivatives play an important role in organic stereochemistry. The Gibbs free energy difference between axial and equatorial conformations in monosubstituted cyclohexanes has been used as a measure of the inherent conformational properties of the substituent. With the rare exception of substituents having mercury bonded to the cyclohexane ring, a general preference for the equatorial conformer is found.<sup>9</sup> Winstein and Holness defined A values as the thermodynamic preference for the equatorial conformation over the axial one (see Scheme 1 for definition of A).<sup>10</sup> Consequently, a positive A value corresponds to a preference for the equatorial conformer. The equatorial preference of alkyl groups as substituents in

## SCHEME 1



cyclohexane has been reinvestigated recently. The A value of the methyl group was found to be 1.80(2) kcal mol<sup>–1</sup> by low-temperature <sup>13</sup>C NMR spectroscopy and 1.98 kcal mol<sup>–1</sup> by ab initio calculations.<sup>11</sup> This is in good agreement with a CCSD(T)/CBS calculated ΔE value of 1.75 kcal mol<sup>–1</sup> by Tschumper et al.<sup>12</sup> Compared to cyclohexane **1**, much less is known about silacyclohexane **6** and its derivatives. The molecular structure of **6** has been determined by gas electron diffraction (GED)<sup>13</sup> and microwave spectroscopy (MW).<sup>14</sup> A theoretical study on the potential energy surface (PES) of **6** has been reported<sup>15</sup> and the path for its chair-to-chair inversion has been calculated.<sup>16</sup>

<sup>&</sup> Conformations of Silicon-Containing Rings. 8. For Part 7 see ref 1.  
<sup>\*</sup> To whom correspondence should be addressed. E-mail: ingvara@raunvis.hi.is.

<sup>†</sup> University of Iceland.

<sup>‡</sup> University of St Andrews.

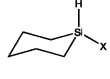
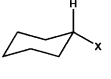
<sup>§</sup> Saint-Petersburgh State Technological Institute.

<sup>||</sup> Technische Universität Graz.

<sup>⊥</sup> Universität Tübingen.

<sup>#</sup> Present address: ICI Rheocenter, Keldnaholti, IS-112 Reykjavik, Iceland.

**TABLE 1: Conformational Properties of Selected Monosubstituted Silacyclohexanes and Cyclohexanes (All Values in kcal mol<sup>-1</sup> and Given as Axial – Equatorial)**

	GED	NMR	Raman	QC <sup>e</sup>		GED	NMR	Raman	QC <sup>e</sup>
	<i>A</i>	<i>A</i>	$\Delta H$	$\Delta E$		<i>A</i>	<i>A</i>	$\Delta H$	$\Delta E$
X = CH <sub>3</sub>	0.45 <sup>a</sup>	0.23 <sup>a</sup>	0.15 <sup>d</sup>	0.12 <sup>f</sup>	X = CH <sub>3</sub>	1.9 <sup>g</sup>	1.6 <sup>j</sup>	<sup>h</sup>	1.70 <sup>f</sup>
X = CF <sub>3</sub>	-0.19 <sup>b</sup>	-0.4 <sup>b</sup>	-0.5 <sup>d</sup>	-0.50 <sup>f</sup>	X = CF <sub>3</sub>	<sup>h</sup>	2.37 <sup>k</sup>	<sup>h</sup>	2.26 <sup>f</sup>
X = F	-0.31 <sup>c</sup>	-0.13 <sup>c</sup>	-0.25 <sup>c</sup>	-0.15 <sup>f</sup>	X = F	0.16 <sup>i</sup>	0.35 <sup>j</sup>	<sup>h</sup>	0.12 <sup>f</sup>

<sup>a</sup> Ref 17. <sup>b</sup> Refs 18 and 19. <sup>c</sup> Ref 1. <sup>d</sup> Ref 20. <sup>e</sup> QC = quantum chemical calculations. <sup>f</sup> Ref 21. <sup>g</sup> Ref 22. <sup>h</sup> Not available. <sup>i</sup> Ref 23. <sup>j</sup> Ref 9. <sup>k</sup> Ref 24.

Reports on monosubstituted silacyclohexanes are rather limited; yet, interesting results have emerged so far. The results from monosubstituted silacyclohexanes with the substituents CH<sub>3</sub>, CF<sub>3</sub>, and F are summarized in Table 1 and compared to the analogous cyclohexanes.

It is striking to see how different these two, so close related, ring systems behave. Not only is the overall equatorial preference of the cyclohexanes greatly diminished in methylsilacyclohexane **7**, moreover is the overwhelming equatorial preference of trifluoromethylcyclohexane **3** turned upside down in trifluoromethylsilacyclohexane **8**. The fluorosilacyclohexane **9** also shows a very different behavior when compared with corresponding cyclohexane **4**. Several recent studies on **5** have been published. The *A* value of the silyl group was found by <sup>1</sup>H and <sup>13</sup>C NMR to be 1.45 and 1.44 kcal mol<sup>-1</sup>, respectively, at 188 K.<sup>25</sup> From a GED experiment, Shen et al. reported a conformational mixture of equatorial (90 ± 10%) and axial forms at 75 °C.<sup>26</sup> Cho et al. have compared calculated *A* values for the methyl and silyl groups.<sup>27</sup> They report *A* values of 2.14 kcal mol<sup>-1</sup> (CH<sub>3</sub>) and 1.90 kcal mol<sup>-1</sup> (SiH<sub>3</sub>) from ab initio calculations, whereas MM3 calculations resulted in 1.78 kcal mol<sup>-1</sup> (CH<sub>3</sub>) and 1.16 kcal mol<sup>-1</sup> (SiH<sub>3</sub>). The authors explained the lower *A* value of the silyl group compared with that of the methyl group by the longer Si–C bond (1.904 Å) compared to the C–C bond (1.534 Å), which makes the axial SiH<sub>3</sub> sterically less unfavorable than the axial methyl group. Durig et al. have recently reported that the equatorial chair of **5** is stabilized by 1.48(20) kcal mol<sup>-1</sup> (temperature-dependent Raman Spectroscopy),<sup>28</sup> 1.18(5) kcal mol<sup>-1</sup> (infrared spectroscopy in Xe solution),<sup>29</sup> and 1.50(3) kcal mol<sup>-1</sup> (MP2 calculations).<sup>29</sup> In this paper, we report on the first synthesis of the silyl substituted silacyclohexane **10** and conformational analysis of that compound by using GED, low-temperature NMR, temperature-dependent Raman spectroscopy, and QC calculations.

## Experimental Section

**Materials.** Silane-*d*<sub>4</sub> was prepared according to a literature procedure.<sup>30</sup> The 1-chloro-1-trichlorosilyl-1-silacyclohexane used as the starting material for the synthesis of 1-silyl-1-silacyclohexane was prepared in slight variation to the general preparation of silacyclohexanes described by West.<sup>31</sup> It should be pointed out that a mixture of chlorinated and brominated substances is obtained by that method because of halogen exchange between the di-Grignard BrMg(CH<sub>2</sub>)<sub>5</sub>MgBr (or the MgBrCl reaction salt) and Cl<sub>3</sub>Si–SiCl<sub>3</sub>, during the reaction. The di-Grignard was prepared in a traditional way. All solvents were dried by using appropriate drying agents and distilled prior to use. Standard

Schlenk technique using dry nitrogen as an inert gas was used for all manipulations. The fact that the end product, 1-silyl-1-silacyclohexane, is a 1,1-disubstituted disilane makes it a potentially hazardous material. We have not encountered any hazards in handling this material, however.

**1-Chloro-1-trichlorosilyl-1-silacyclohexane.** BrMg(CH<sub>2</sub>)<sub>5</sub>MgBr (28.5 g, 102.3 mmol) was slowly added to Cl<sub>3</sub>Si–SiCl<sub>3</sub> (25.0 g, 93.0 mmol) dissolved in Et<sub>2</sub>O (100 mL) while stirring at 0 °C. A lot of gray reaction salt was formed during the reaction. After stirring overnight, the Et<sub>2</sub>O was distilled off the reaction mixture and replaced by pentane. The reaction mixture was then filtered under nitrogen, and the salt was discarded. Distillation under reduced pressure (110–111 °C, 5 Torr) yielded 17.6 g (65.6 mmol, 71%) of 1-chloro-1-trichlorosilyl-1-silacyclohexane, which contained 25–30% of partly brominated products.

**1-Silyl-1-silacyclohexane.** 1-Chloro-1-trichlorosilyl-1-silacyclohexane (12.8 g, 47.7 mmol) dissolved in Et<sub>2</sub>O (60 mL) was slowly added to a suspension of LiAlH<sub>4</sub> (2.1 g, 54.9 mmol) in Et<sub>2</sub>O (80 mL) while stirring at 0 °C. After boiling for 12 h, most of the Et<sub>2</sub>O was removed from the solution and replaced by pentane. The reaction mixture was filtered under nitrogen, and the salt was discarded. All volatile components were then condensed to a N<sub>2</sub>(*l*) cooled finger. The desired product was then collected by distillation at 131–132 °C and 500 Torr. Further purification was achieved by preparative GC, attaining an analytically pure colorless liquid confirmed by NMR spectroscopy. Yield: 3.84 g (29.5 mmol, 60%); <sup>1</sup>H NMR (400 MHz, CDCl<sub>3</sub>): δ 0.76–0.84 (m, 2H, CH<sub>2(ax/eq)</sub>), 0.93–1.00 (m, 2H, CH<sub>2(ax/eq)</sub>), 1.39–1.52 (m, 2H, CH<sub>2</sub>), 1.68–1.82 (m, 4H, CH<sub>2</sub>), 3.09 (d, 3H, <sup>3</sup>J<sub>H–H</sub> = 3 Hz, <sup>1</sup>J<sub>Si–H</sub> = 190 Hz, SiH<sub>3</sub>), 3.91–3.95 (m, 1H, SiH) ppm. <sup>13</sup>C NMR (101 MHz, CDCl<sub>3</sub>): δ 9.6, 25.6, 29.6 (CH<sub>2</sub>) ppm. <sup>29</sup>Si NMR (79 MHz, CDCl<sub>3</sub>): δ -97.2 (s, SiH), -102.0 (s, <sup>1</sup>J<sub>Si–Si</sub> = 77 Hz, SiH<sub>3</sub>) ppm. HRMS (EI, 70 eV): *m/z* found 130.0627, calcd. for C<sub>5</sub>H<sub>14</sub>Si<sub>2</sub> 130.0634.

**GED Experiment.** Electron-diffraction intensities were recorded at Moscow State University with an EG-100A electron-diffraction unit at 194 and 362 mm nozzle-to-plate distances and with an accelerating voltage of about 60 kV.<sup>32</sup> The electron wavelength was derived from diffraction patterns of gaseous CCl<sub>4</sub>, and was 0.05012 and 0.05001 Å, and the nozzle temperature was 65 and 48 °C for short and long nozzle-to-plate distances, respectively. The photographic films (Kodak, 12 × 9 cm) were analyzed with an Epson 4870 scanner, and total scattering intensity curves were obtained by using the program written by A. V. Belyakov. Experimental backgrounds were drawn as least-squares adjusted polynomials to the

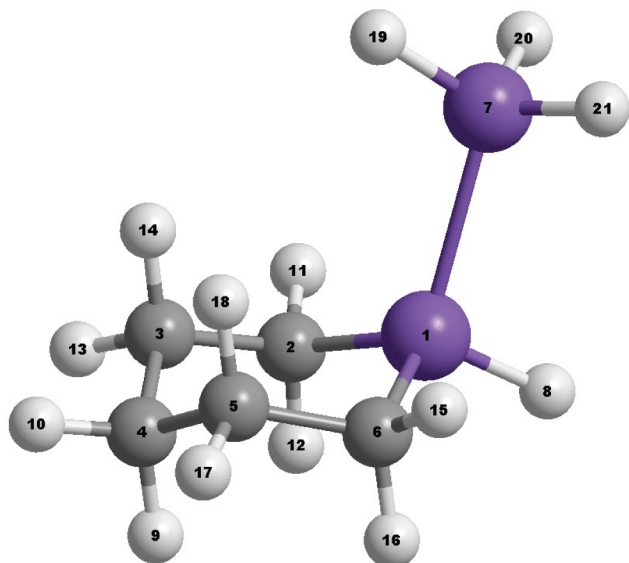


**Figure 1.** Structural model of the axial (**10a**) conformer of **10** with atom numbering.

difference between the total experimental intensity and molecular intensities calculated from the best geometrical model by using a program written by A. V. Belyakov. Averaged experimental molecular intensities in the range  $s = 3\text{--}18.6$  and  $18.2\text{--}30.0 \text{ \AA}^{-1}$  in steps of  $\Delta s = 0.2 \text{ \AA}^{-1}$  for short and long nozzle-to-plate distances, respectively, ( $s = (4\pi/\lambda) \sin \theta/2$ , where  $\lambda$  is the electron wavelength and  $\theta$  is the scattering angle) are available as Supporting Information. Weight matrices were diagonal, the 362 mm data were assigned unit, and the 194 mm data were half weight.

**Low-Temperature NMR Experiment.** A NMR sample using  $\text{SiD}_4$  as solvent was prepared for the low-temperature  $^{13}\text{C}$  NMR measurements. The solvent served as lock signal as well. CAUTION: A probe like this must be handled with great care and should never be allowed to warm up above 200 K. The temperature of the probe was calibrated by means of a type K (Chromel/Alumel) thermocouple inserted into a dummy tube the day before and the day after the NMR experiment. The readings are estimated to be accurate within  $\pm 2$  K. The NMR

spectra were loaded into the data-handling program IGOR (WaveMetrics) for analysis, manipulations, and graphic display. Line-shape simulations of the NMR spectra were performed by using the WinDNMR program.<sup>33</sup>

**Low-Temperature Raman Experiment.** Raman spectra were recorded with a Jobin Yvon T64000 spectrometer equipped with a triple monochromator and a CCD camera. The samples were filled into 1 mm capillary glass tubes and irradiated by the green 532 nm line of a frequency doubled Nd:YAG Laser (Coherent, DPSS model 532-20, 10 mW). Spectra were recorded from pure compound and in heptane and THF solution. A continuous flow cryostat, Oxford instruments OptistatCF<sup>TM</sup>, using liquid nitrogen for cooling, was employed for the low-temperature measurements.

## Results and Discussion

**GED Analysis.** Structure refinements of compound **10** were carried out with least-squares analyses of the experimental molecular intensity curve  $sM(s)$ . According to quantum chemical calculations, two stable conformers of  $\text{C}_3\text{H}_{10}\text{SiHSiH}_3$  exist, axial (**10a**) and equatorial (**10e**). Each form possesses  $C_s$  symmetry with chair conformation of the six-membered ring. Figure 1 shows the molecular structure of **10a** along with atom numbering. Figure 2 compares observed and calculated radial distribution  $f(r)$  curves for the mixture of axial and equatorial conformers. Analysis of radial distribution curves separately for axial and equatorial conformers revealed that remarkable differences exist in the region  $r > 2.8 \text{ \AA}$  that correspond to the peaks of conformation dependent nonbonded  $\text{C}\cdots\text{Si}(7)$  distances (Figure 2). This demonstrates that the electron-diffraction intensities are sensitive toward the conformational properties of this compound. Comparison with the experimental radial distribution function  $f(r)$  which was derived by Fourier transformation of the molecular intensities testifies that both conformers are present in the vapor under the conditions of the electron-diffraction experiment in nearly equal quantities.

Least-squares refinement of the structural parameters was performed with the use of a modified version of the KCED25 M computer program.<sup>34,35</sup> Scattering amplitudes and phases of ref 36 were used. The geometry of the six-membered ring was described by three bond lengths (Si–C2, C2–C3, and C3–C4), two bond angles (C2–Si–C6 and C3–C4–C5), and the two

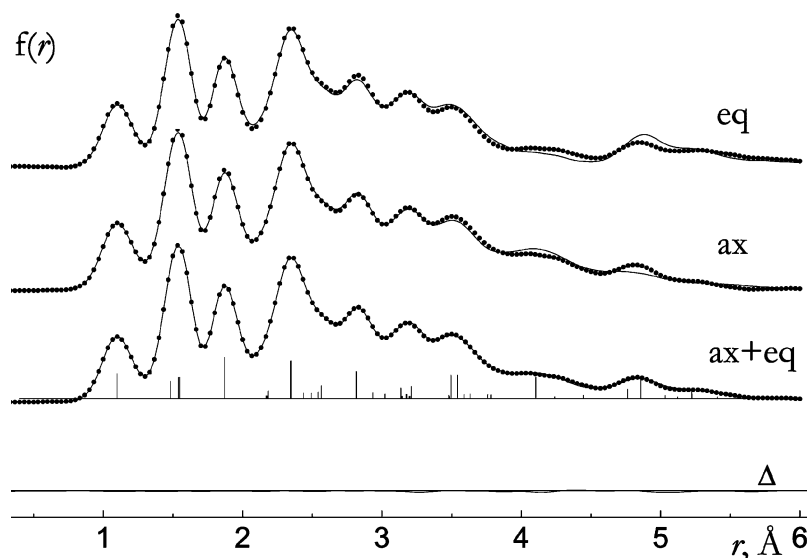


**Figure 2.** Radial distribution functions for the mixture of axial and equatorial conformers (experimental, dots; calculated, full line). Refinements are shown for the axial and equatorial conformer separately and for the mixture. At the bottom is the difference curve for the mixture.

**TABLE 2: Experimental and Calculated Geometric Parameters of Axial Conformer of C<sub>5</sub>H<sub>10</sub>SiHSiH<sub>3</sub> (in Angstroms and Degrees, C<sub>s</sub> Symmetry)<sup>a</sup>**

	<i>r</i> <sub>a(angles-h1)</sub> structure	<i>r</i> <sub>e</sub> structure			
	GED	B3LYP/6-31G(d,p)	MP2/6-31G(d,p)	MP2/cc-pVTZ	M06-2X/pc-2
Si-C <i>p</i> <sub>1</sub> <sup>b</sup>	1.872(2)	1.903	1.893	1.890	1.883
Si-Si <sub>ax</sub> <i>p</i> <sub>2</sub>	2.348(3)	2.360	2.347	2.356	2.344
Si-Si <sub>eq</sub> ( <i>p</i> <sub>2</sub> )	2.343(3)	2.355	2.342	2.352	2.339
C2-C3 <i>p</i> <sub>3</sub>	1.548(3)	1.545	1.537	1.537	1.537
C3-C4 ( <i>p</i> <sub>3</sub> )	1.541(3)	1.540	1.532	1.530	1.531
(C-H) <sub>mean</sub> <i>p</i> <sub>4</sub>	1.102(2)	1.098	1.093	1.093	1.092
Si-H <sub>mean</sub>	1.482(7)	1.492	1.481	1.485	1.481
Si-Si-H	108.8 <sup>c</sup>	107.5	108.7	108.8	108.6
C2-Si-C6 <i>p</i> <sub>5</sub>	103.7(4)	104.1	103.6	103.9	104.2
C3-C4-C5 <i>p</i> <sub>6</sub>	111.1(8)	114.6	114.4	114.2	114.2
Si-Si-X1 <sub>ax</sub> <i>p</i> <sub>7</sub>	132.1(15) <sup>d</sup>	127.9	125.8	125.8	124.3
Si-Si-X1 <sub>eq</sub> <i>p</i> <sub>8</sub>	127.0(17)	130.2	129.5	129.5	128.8
(H-C-H) <sub>mean</sub>	106.4 <sup>c,e</sup>	106.1	106.4	106.5	106.5
flap(Si) <sub>ax</sub> <i>p</i> <sub>9</sub>	41.4(16)	39.9	42.8	42.8	42.8
flap(Si) <sub>eq</sub> ( <i>p</i> <sub>9</sub> )	41.6(16)	41.1	43.0	43.0	42.9
flap(C4) <i>p</i> <sub>10</sub>	59.6(7)	56.6	57.4	57.4	57.8
<i>R</i> factor, (%)	3.7				

<sup>a</sup> Atom numbering is given in Figure 1. Error limits are  $3\sigma_{LS}$  values. <sup>b</sup> *p*<sub>*i*</sub>, refined parameter; (*p*<sub>*i*</sub>), the difference with parameter *p*<sub>*i*</sub> was set to MP2/cc-pVTZ calculated value; if not specified, the observed parameter is the average for two conformers. <sup>c</sup> Not refined. <sup>d</sup> X<sub>*i*</sub>, dummy atom on the bisector of the adjacent endocyclic angle. <sup>e</sup> H<sub>ax</sub>-C2-C3 = H<sub>eq</sub>-C3-C2 = H<sub>eq</sub>-C3-C4 = H<sub>ax</sub>-C3-C2.

**TABLE 3: Interatomic Distances, Experimental and Calculated Vibrational Amplitudes and Vibrational Corrections (Without Non-Bonded Distances Involving Hydrogen Atoms) for Axial Conformer of C<sub>5</sub>H<sub>10</sub>SiHSiH<sub>3</sub> (in Angstroms)<sup>a</sup>**

	<i>r</i> <sub>a</sub>	<i>l</i> <sub>exp</sub>	<i>l</i> <sub>calc</sub> <sup>b</sup>	$\Delta r = r_{h1} - r_a$	group <sup>c</sup>
C-H	1.102(2)	0.081(2)	0.076	0.0016	1
C2-C3	1.548(3)	0.056(2)	0.052	0.0007	1
C3-C4	1.541(3)	0.056(2)	0.051	0.0006	1
Si-H	1.482(7)	0.093(2)	0.088	0.0017	1
Si-C2	1.872(2)	0.057(2)	0.053	0.0005	1
Si-Si	2.348(3)	0.062(2)	0.057	0.0003	1
C2...C4	2.573(7)	0.072(2)	0.072	0.0048	2
C3...C5	2.538(13)	0.070(2)	0.070	0.0049	2
Si1...C3	2.819(6)	0.078(2)	0.077	0.0062	2
C2...C6	2.941(9)	0.087(2)	0.087	0.0050	2
C2...Si7	3.547(16)	0.130(2)	0.130	0.0115	2
C2...C5	3.137(6)	0.084(2)	0.084	0.0076	2
Si1...C4	3.216(10)	0.079(2)	0.078	0.0087	2
C3...Si7	4.130(35)	0.206(2)	0.206	0.0204	2
C4...Si7	4.793(40)	0.194(2)	0.193	0.0242	2

<sup>a</sup> Atom numbering is given in Figure 1. Error limits are  $3\sigma_{LS}$  values. <sup>b</sup> MP2/cc-pVTZ. <sup>c</sup> Group of refined amplitudes.

flap angles between the C2SiC6 (flap(Si)) or C3C4C5 plane (flap(C4)) and the C2C3C5C6 plane. The orientation of the Si-Si and C4-H<sub>ax</sub> bonds is described by two dummies X1 and X2, situated on the bisector of the adjacent endocyclic angles C2-Si-C6 and C3-C4-C5, respectively. To reduce the number of refined parameters, the following assumptions were made on the basis of MP2 results. Only the geometric parameters of the axial conformer were refined, and the parameters of the equatorial form were tied to those of the axial conformer by using the calculated differences. For the axial conformer, the difference between the nearly equal C2-C3 and C3-C4 bond lengths was constrained to the calculated value. All C-H bonds, H-C-H angles, and H<sub>ax</sub>-C2-C3, H<sub>eq</sub>-C3-C2, H<sub>eq</sub>-C3-C4, and H<sub>ax</sub>-C3-C2 angles are set equal. Angles that define the orientation of the C-H bonds were set to the calculated values. Theoretical values for geometrical parameters and vibrational amplitudes were used as initial approximation. Cartesian coordinates of atoms were calculated in terms of a geometrically

consistent *r*<sub>h1</sub> structure. Mean amplitudes and shrinkage corrections *r*<sub>h1</sub> - *r*<sub>a</sub> were calculated from MP2 force constants with the SHRINK program which takes nonlinear transformation of internal and Cartesian coordinates into account.<sup>37,38</sup> In the least-squares refinement, the vibrational amplitudes were divided into two groups, one group for bonded and the other one for nonbonded distances. In each group, amplitudes were refined with fixed differences from MP2 calculations. With the above assumptions, ten structural parameters (see Table 2), two groups of vibrational amplitudes, the mole fraction of the axial conformer, and two scale factors were refined simultaneously. The final values of refined parameters are presented in Tables 2 and 3. In spite of the above assumptions, a remarkable correlation existed between the following parameters: C(2)SiC(6)/flap(Si(1)) = -84%. According to the GED data, the concentration of the axial conformer **10a** in the vapor of **10** at 321 K is 57(7) mol %. This value corresponds to an *A* value of -0.17(15) kcal mol<sup>-1</sup> (Table 4).

**NMR Spectroscopy.** Because of limited solubility of **10**, no signal separation could be observed in the <sup>13</sup>C NMR spectra of **10** at low temperatures when using a solvent mixture of CD<sub>2</sub>Cl<sub>2</sub>, CHFCl<sub>2</sub>, and CHF<sub>2</sub>Cl in a ratio of 1:1:3, which we have successfully used in previous studies.<sup>1,17,18</sup> A new sample was prepared by using SiD<sub>4</sub> as the solvent, which also provided the lock signal. As far as we know, silane or silane-*d*<sub>4</sub> has not been used as NMR solvent before. CAUTION: It has to be emphasized that silane must be handled with great care, considering its volatile and pyrophoric nature. The SiD<sub>4</sub> sample allowed us to record <sup>13</sup>C NMR spectra of **10** down to 100 K. At 164 K and down to about 130 K, the <sup>13</sup>C NMR spectra show rapid interconversion of **10e** and **10a**. On cooling below 130 K, the spectrum (Figure 3) shows large line broadening and gradual splitting of signals into two components of similar magnitude, indicating a mixture of two conformers. In a previous work on **7**, we have shown that the <sup>13</sup>C chemical shifts of the ring carbon atoms have lower  $\delta$  values when the substituent is in the axial position than when it is in the equatorial one.<sup>17</sup> On the basis of the <sup>13</sup>C NMR signal weights (hence relative populations) and QC chemical shift calculations for **10e** and **10a**, we conclude that the same holds for the C2(6) and C3(5) ring carbon atoms

TABLE 4: Conformational Properties of C<sub>3</sub>H<sub>10</sub>SiHSiH<sub>3</sub>

method/basis set <sup>a</sup>	T = 0 K	T = 300–210 K	T = 110 K	T = 321 K
	$\Delta E = E_{ax} - E_{eq}$ kcal mol <sup>-1</sup>	$\Delta H = H_{ax} - H_{eq}$ kcal mol <sup>-1</sup>	$A = G_{ax} - G_{eq}$ kcal mol <sup>-1</sup>	$A = G_{ax} - G_{eq}$ kcal mol <sup>-1</sup>
	Calculations			
CCSD(T)/CBS	0.04	0.05	0.09	0.14
MP2/CBS	-0.04	-0.02	0.02	0.06
M06-2X/pc-3	-0.14	-0.12	-0.08	-0.04
B2PLYP-D/QZVPP	0.11	0.12	0.16	0.21
B3LYP/pc-3	0.74	0.76	0.79	0.84
	Experiment			
GED				-0.17(15)
Raman, neat		-0.26(10)		
Raman, in THF		-0.23(10)		
Raman, in heptane		-0.22(10)		
NMR			0.05(3)	

<sup>a</sup> All calculations are single-point energies at M06-2X/pc-2 geometries. Zero-point energy and enthalpic and entropic corrections (at nonzero temperatures) calculated at the B97-1/pc-2 level for all cases. <sup>b</sup> Values are zero-point energy exclusive.

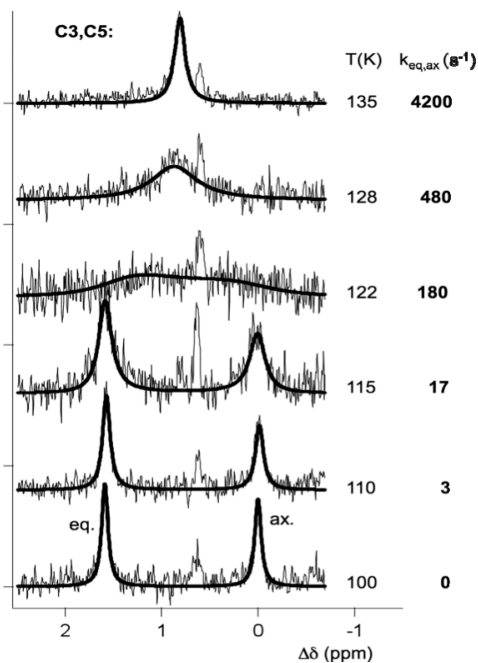


**Figure 3.** Simulation of the <sup>13</sup>C NMR signals for C3 and C5 in a solution of SiD<sub>4</sub> at low temperatures. The simulation ignores a small signal due to impurities.

for **10**. The resonance signals for C4 (**10**) in the axial position, on the other hand, are found to have slightly higher  $\delta$  value than that for the equatorial position. The results of the <sup>13</sup>C chemical shift calculations are given in more details in a separate section below. Dynamic NMR simulations of the spectra, performed by using the software WinDNMR<sup>33</sup> as shown in Figure 3, allowed us to determine the rate constants and the corresponding free energies of activation as a function of temperature. The most reliable results were obtained from the C3(5) pair of carbon atoms. Thus,  $\Delta G_{e \rightarrow a}^\ddagger = 5.7(2)$  kcal mol<sup>-1</sup> was obtained for about 124 K. Furthermore, the equilibrium constant (hence free energy changes) for the equatorial-to-axial transformations, corresponding to temperatures slightly lower than the coalescence-point temperature (about 110 K), could be determined from the relative signal intensities ( $K_{e \rightarrow a} = 0.8$  and  $\Delta G_{e \rightarrow a} = +0.05$  kcal mol<sup>-1</sup>). The derived rate constants indicate slightly decreasing  $\Delta G_{e \rightarrow a}^\ddagger$  values with temperature in the 110–138 K range. More information is given as Supporting Information.

**Raman Spectroscopy.** To analyze temperature-dependent Raman spectra of a compound possessing two conformational

minima, I and II, the van't Hoff relation  $\ln(A_I/A_{II}) = -\Delta H/RT + \text{constant}$  is used.  $A_I$  and  $A_{II}$  are the intensities of lines (either peak heights or peak areas) originating from conformer I and II of the compound. The enthalpy difference  $\Delta H$  is obtained from the slope of the plot  $\ln(A_I/A_{II})$  against  $T^{-1}$ . The van't Hoff equation in the form given above is derived under the assumption that  $\Delta H (= H_I - H_{II})$  and the Raman scattering coefficients for conformers I and II are independent of temperature.

To obtain accurate  $\Delta H$  values with this method, it is important that the bands of conformers I and II possess reasonable intensity, sit on a flat baseline, and do not overlap with other bands of the spectrum. As discussed in a paper by Klaeboe,<sup>39</sup> there is an additional requirement, which is even more important. The bands used for the van't Hoff plot have to be pure bands, which means that their intensities must be due to one conformer only. If this is not the case, a systematic error will be introduced which in most cases cannot be quantified, unless one conformer disappears completely from the mixture at low temperature. Therefore, more than one pair of bands should be used whenever possible. If considerable discrepancies occur between  $\Delta H$  values deduced from different pairs, it is a sure sign that not all bands employed for the van't Hoff plots are pure.

Impurity of a band in the sense discussed above very often results from overtone or combination bands of one conformer overlapping with a fundamental band of the other conformer. Because the number of possible overtones and combinations normally is quite large and some of them might be enhanced by the ever-present Fermi resonance, even consistent  $\Delta H$  values from two or more band pairs do not necessarily guarantee a correct  $\Delta H$  value. This is discussed in ref 39 for the case of *n*-butane. In the Raman spectrum of the vapor, two band pairs giving  $\Delta H$  values of  $1.09 \pm 0.10$  and  $1.13 \pm 0.16$  kcal mol<sup>-1</sup> were identified (quoted from ref 39,  $\Delta H$  values converted to kcal mol<sup>-1</sup>). The correct value seems to be 0.69 kcal mol<sup>-1</sup>, obtained from several independent methods. This may serve as an example that in many IR and Raman investigations, the systematic error is much larger than the statistical error, often by a factor of 4–5 or even more.

The Raman spectrum of the pure compound in the wave-number range 150–2200 cm<sup>-1</sup> is shown in Figure 4, including the expanded range of the Si–Si and Si–C stretching vibrations from 350 to 700 cm<sup>-1</sup>. According to QC calculations, the two bands at 414 and 432 cm<sup>-1</sup> were assigned to the Si–Si stretching modes, and the two bands at 637 and 652 cm<sup>-1</sup> were assigned to the symmetric Si–C stretching modes ( $A'$ ) in **10a** and **10e**, respectively (B3LYP/6-31G(d,p) calculation: **10a** = 409/626

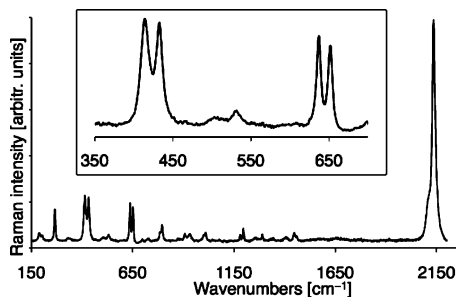


**Figure 4.** Raman spectrum at 300 K of neat liquid  $C_5H_{10}SiHSiH_3$  in the wavenumber range 150–2200  $cm^{-1}$ . The range 350–700  $cm^{-1}$ , which includes the conformation-sensitive Si–Si and Si–C stretching vibrations, has been expanded for illustrative purposes.

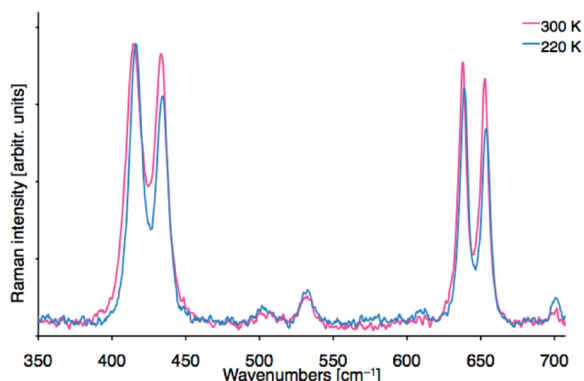


**Figure 5.** Appearance of the line pairs of the Si–Si stretching (414/432  $cm^{-1}$ ) and the Si–C stretching vibrations (637/652  $cm^{-1}$ ) of a THF solution of  $C_5H_{10}SiHSiH_3$  at 300 K (red) and 220 K (blue).

$cm^{-1}$ ; **10e** = 427/639  $cm^{-1}$ ). In the neat liquid as well as in solutions in THF or *n*-heptane, both band pairs show almost identical variations of the intensity ratio with temperature, proving that they result from a conformational equilibrium. For the THF solution, the appearance of the two band pairs (414/432 and 637/652  $cm^{-1}$ ) for 300 and 220 K is presented in Figure 5, illustrating the intensity changes that have been observed.

For the pure liquid, the THF solution, and the *n*-heptane solution, both band pairs were analyzed in the temperature range 300–210 K in 15 K steps. Van't Hoff plots obtained by employing either peak heights or band areas for the calculation of intensity ratios show that peak heights produce much more consistent results, with  $\Delta H$  ( $= H_{ax} - H_{eq}$ ) values in the range  $-0.29 < \Delta H < -0.19$  kcal mol $^{-1}$ . Moreover, regression coefficients  $R^2$  generally are larger than 0.96 for peak heights but are considerably smaller for peak areas (though not in all cases). For the band pair 414/432  $cm^{-1}$  in *n*-heptane solution, even a positive sign for  $\Delta H$  is obtained when using band areas. This certainly is due to a weak solvent peak located at  $\sim 400$   $cm^{-1}$ , which broadens the base of the 414  $cm^{-1}$  peak but does not increase its height. In addition, peak areas are notoriously inaccurate for overlapping peaks, because they have to be determined by band deconvolution. Figure 6 presents typical van't Hoff plots for the band pair 637/652  $cm^{-1}$  (*n*-heptane solution) obtained by using both peak heights and peak areas.

We present  $\Delta H$  values for peak heights only which we think are more accurate because peak maxima in both band pairs are well separated (Figure 5). For the two band pairs (414/432 and 637/652  $cm^{-1}$ ), the following  $\Delta H$  values were obtained: neat liquid,  $-0.329/-0.185$  kcal mol $^{-1}$ ; THF solution,  $-0.259/-0.192$  kcal mol $^{-1}$ ; heptane solution,  $-0.221/-0.221$  kcal mol $^{-1}$ . Mean values are  $-0.26$  kcal mol $^{-1}$  for the pure liquid,  $-0.23$  kcal mol $^{-1}$  for the THF solution, and  $-0.22$  kcal mol $^{-1}$

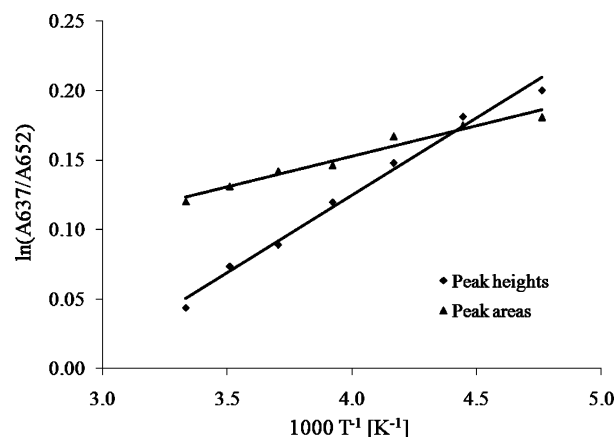


**Figure 6.** Van't Hoff plot for the band pair 637/652  $cm^{-1}$  (*n*-heptane solution) obtained by using band areas (triangles) and band heights (diamonds).

for the heptane solution as summarized in Table 4. The confidence intervals (95%) calculated from the data points for each band pair are about  $\pm 0.03$  kcal mol $^{-1}$  for all solvents. As stated previously, systematic errors often are 3–5 times larger. We therefore believe that a value of about  $\pm 0.1$  kcal mol $^{-1}$  is much more reasonable as error limit. Quite remarkably, the polarity of the solvents does not significantly influence  $\Delta H$ .

**Computational Studies in the Gas Phase.** The minimum-energy pathway for the chair-to-chair inversion of silylsilacyclohexane **10** has been calculated in a redundant internal coordinate system with the STQN(Path) method as implemented in Gaussian03<sup>40</sup> at the B3LYP/6-311+G(d,p) level of theory. Similarly to the trifluoromethyl derivative **7**,<sup>18</sup> the path was calculated in four slices by using the keyword OPT(QST3,PATH=11), that is from minimum **10a** to **10b**, from **10b** to **10c**, from **10c** to **10d**, and from **10d** to **10e**, as shown in Figure 7. The inversion path from the axial conformer, **10a**, consists of a half-chair/sofa-like transition state from which the molecule can move into a twist form of relatively high energy (**10b**). The molecule then goes through a boat form into a more stable twist form (**10c**) at the midpoint of the path. The molecule then proceeds further through a boat transition state, a twist minimum (**10d**), and a half-chair/sofa transition state before it ends up in the equatorial form, **10e**.

Geometry optimization of the axial and equatorial conformers was performed with several methods for direct comparison with geometric data from the GED experiment (Table 2). The M06-2X density functional<sup>41,42</sup> with the pc-2<sup>43,44</sup> basis set (triple- $\zeta$  quality) gives bond lengths and angles in good agreement with experiment, and M06-2X/pc-2 geometries were subsequently used for single-point energy calculations.

Several single-point energy calculations were carried out by using both DFT and ab initio methods to get energy differences between the axial and equatorial conformers, shown in Table 4.

Previous experience alerted us to the failure of popular DFT methods to predict accurate conformational energy differences.<sup>21</sup> We thus set out to calculate very accurate complete basis-set estimates at the CCSD(T) level, a method often referred to as the golden standard of quantum chemistry. This involves doing large basis MP2 calculations that are then extrapolated to the basis-set limit and then calculating a CCSD(T) correction ( $\delta$ ) to the MP2/CBS value. This has been shown to be a good way to obtain CCSD(T)/CBS estimates because the correction converges rather quickly with increasing basis set.<sup>45</sup> This method has previously been used to calculate CCSD(T)/CBS  $\Delta E$  values

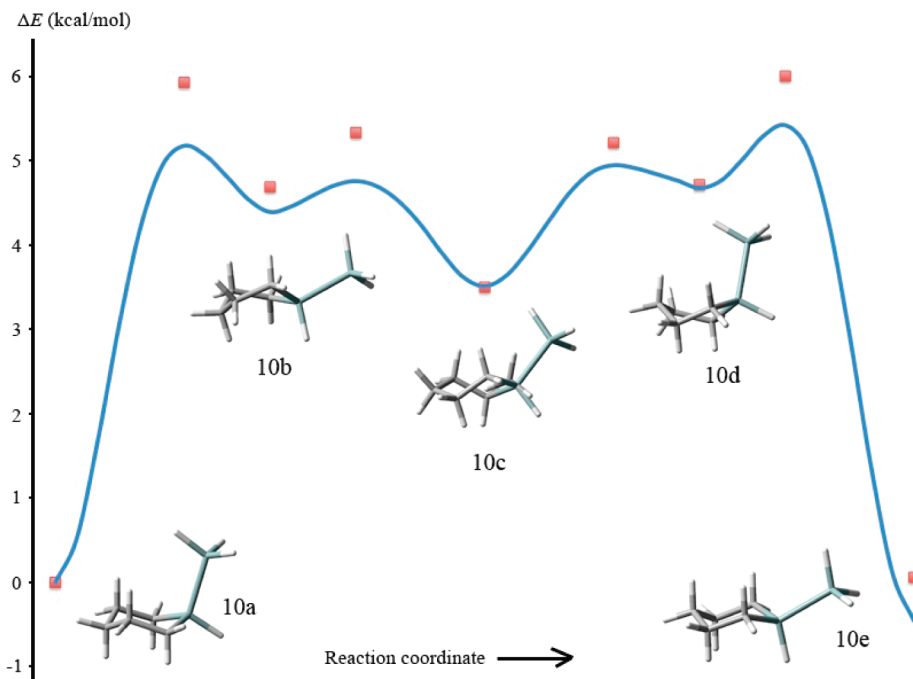


**Figure 7.** B3LYP/6-311+G(d,p) minimum-energy pathway for the chair-to-chair inversion of silylsilacyclohexane **10**. Squares are M06-2X/pc-2//B3LYP/6-311+G(d,p) energies.

**TABLE 5: Convergence of the  $\delta$  Correction Used in the  $\Delta E$  CCSD(T)/CBS Estimate<sup>a</sup>**

basis set	$\Delta E^{\text{CCSD(T)}}$	$\Delta E^{\text{MP2}}$	$\delta = \Delta E^{\text{CCSD(T)/basis}} - \Delta E^{\text{MP2/basis}}$
cc-pVDZ	0.239	0.159	0.080
aug-cc-pVDZ	-0.142	-0.201	0.059
cc-pVTZ	0.033	-0.042	0.075
aug-cc-pVTZ	-0.007	-0.080	0.073

<sup>a</sup> All values in kcal mol<sup>-1</sup>.

of similar systems.<sup>12,46</sup> The following formulas show how the CCSD(T)/CBS estimate was calculated:

$$\Delta E^{\text{CCSD(T)/CBS}} = \Delta E^{\text{MP2/CBS}} + \delta$$

$$\delta = \Delta E^{\text{CCSD(T)/small basis}} - \Delta E^{\text{MP2/small basis}}$$

MP2 calculations were done with the correlation-consistent basis sets<sup>47,48</sup> up to the cc-pV5Z level and were extrapolated to the basis-set limit by separate extrapolation of HF energies (T,Q,5) and MP2 correlation energies (T,Q,5) by the extrapolation scheme of Helgaker.<sup>49</sup> The CCSD(T)  $\delta$  correction term was calculated at several different levels to ensure the convergence of the correction, shown in Table 5. The correction calculated with the largest basis set (aug-cc-pVTZ) was then added to the MP2/CBS value.

Recent density functionals, like M06-2X<sup>41,42</sup> and B2PLYP-D,<sup>50,51</sup> have been shown to yield reliable energetics of organic and main-group molecules. Single-point energy calculations at the M06-2X/pc-3 level and the B2PLYP-D/def2-QZVPP level were performed and compared to the well-known B3LYP functional. Large basis sets of the quadruple- $\zeta$  level (pc-3 and def2-QZVPP<sup>52</sup>) were used that ensured converged energy differences.

The enthalpy and entropy corrections to the conformational energies were all done at the same level for consistency, B97-1/pc-2. The B97-1 functional<sup>53</sup> is known to predict good harmonic frequencies and enthalpy and entropy corrections.<sup>54</sup> We did several frequency calculations with the B97-1 functional

and found that the entropy correction was quite sensitive to basis-set effects as well as convergence criteria and integration grid. B97-1 with the pc-2 basis set and tight convergence criteria and ultrafine grid in Gaussian was found to predict consistent results. It should be pointed out, however, that our B97-1/pc-2 corrections are based on the harmonic oscillator approximation. Six-membered rings include a number of low-frequency vibrations that are known to be badly predicted by the harmonic approximation. Because these vibrations contribute significantly to entropy, errors in the free-energy correction can be expected. This problem has been noted recently in the literature for another ring system, cyclooctane,<sup>55</sup> and for substituted ethanes,<sup>56</sup> where the failure of the harmonic approximation to properly describe low-frequency vibrations was found to greatly affect the thermal contribution to entropy and, hence, the free-energy difference of conformers. The low-frequency internal rotation mode involving the SiH<sub>3</sub> group of **10** can be described as a hindered rotor following work by various groups,<sup>57–60</sup> and the total vibrational partition function can hence be corrected, by the freq=HinderedRotor keyword in the Gaussian program. This procedure gives only an additional 0.01 kcal/mol correction to the relative harmonic free-energy correction. A solid method to account for other low-frequency vibrations (for example, ring torsional modes) does not exist, and we are therefore unfortunately relying on cancellation of errors.

Shown in Table 4 are calculated relative energies with thermodynamical corrections at experimental temperatures compared to the experimental (GED, Raman, NMR) energy differences. The CCSD(T)/CBS value is considered to be the most accurate theoretical estimate of the electronic energy difference,  $\Delta E$  (ZPE excluded at 0 K). Here, the conformers are approximately equally stable, the equatorial conformer being slightly more favorable by 0.04 kcal/mol. Zero-point energy and thermal corrections to enthalpy at higher temperature are small (0.01 kcal/mol), whereas the entropic correction becomes slightly more important as temperature increases and stabilizes the equatorial conformer further (0.05 kcal/mol at 110 K and 0.10 kcal/mol at 321 K).

**TABLE 6: Calculated Relative  $^{13}\text{C}$  Chemical Shifts (Relative to TMS) in **10a** and **10e** (ppm) Compared to Experimental Chemical Shifts from DNMR at 100 K**

atoms	<b>10a</b>	<b>10e</b>	difference ( <b>10e</b> – <b>10a</b> )
		GIAO	
C2 + C6	12.0	13.1	1.1
C3 + C5	27.7	29.4	1.7
C4	32.7	32.5	-0.2
		Experiment	
C2 + C6	10.3	11.3	1.0
C3 + C5	26.3	27.9	1.6
C4	30.9	30.8	-0.1

The Raman results indicate a slightly higher population of the axial conformer and are thus in slight disagreement with the  $\Delta H$  CCSD(T) estimate. The GED free-energy difference also shows the axial conformer to be more stable. The NMR results at 110 K on the other hand are in excellent agreement with the  $\Delta G$  CCSD(T) estimate at the same temperature. We note that solvent effects are not taken into account in these calculations. The Raman experiments suggest very small solvent effects on  $\Delta H$ . Simple single-point calculations with the PCM<sup>61</sup> solvation model in heptane and THF solution confirm these observations, although the IPCM<sup>62</sup> model shows slightly different results. See Supporting Information.

We also note the failure of the B3LYP functional to account for the energy difference between the conformers. The B3LYP value is in significant disagreement with both the experimental values and the CCSD(T)/CBS value. Recent DFT methods, M06-2X and B2PLYP-D, have been shown to account for dispersion interactions far much better and can be recommended for exploring conformational properties of similar molecules. The ability of these DFT methods to predict conformational energy differences in good agreement with CCSD(T)/CBS values has been demonstrated recently.<sup>21</sup> Finally, the free energy of activation of the chair-to-chair inversion,  $\Delta G^\ddagger_{e-a} = 5.79$  kcal/mol was calculated at the M06-2X/pc-2 level with B97-1/pc-2 thermal corrections at 124 K. This is in excellent agreement with the DNMR value of  $\Delta G^\ddagger_{e-a} = 5.7(2)$  kcal/mol.

**$^{13}\text{C}$  NMR Shieldings.** The absolute shielding constants of the carbon nuclei were calculated with the GIAO<sup>63,64</sup> method by using PBE1PBE/6-311+G(2pd).<sup>65</sup> All geometries (including the TMS standard) were optimized at the M06-2X/pc-2 level. The magnitude of the relative shieldings is in excellent agreement with experiment, and their sign confirms the expected assignment in which the ring carbon nuclei (apart from C4) are more shielded in the axial conformer than in the equatorial one (Table 6).

## Conclusions

The conformational properties of methyl-, trifluoromethyl-, and fluorosilacyclohexane have previously been reported and compared with their cyclohexane analogues.<sup>1,17–19</sup> In all cases, the preference for the equatorial chair form, which has been established for the cyclohexane derivatives, is greatly diminished or even turned upside down for the silacyclohexanes. Silylcyclohexane, too, has a clear preference for the equatorial form. According to three different experiments reported herein, silylsilacyclohexane has a slight preference for the axial form (GED, Raman), or the two conformers are almost equally populated (DNMR). Hence, the silyl group in silylsilacyclohexane shows no preference for the equatorial position, contrary to what is found for silylcyclohexane. Our results demonstrate that it is difficult to reproduce the experimental results for

silylsilacyclohexane exactly by quantum chemical calculations. Even in the case of high-level CCSD(T)/CBS and MP2/CBS calculations, one has to accept a deviation from experimental results in the magnitude of 0.1–0.3 kcal mol<sup>-1</sup>. These deviations may partly be due to assumed harmonicity of low-frequency vibrations, resulting in erroneous entropic corrections (at the B97-1/pc-2 level). Two recent DFT functionals that take into account dispersion interaction also performed satisfactory, whereas the popular B3LYP functional predicted unacceptable results.

**Acknowledgment.** A financial support from Rannís—The Icelandic Centre for Research is gratefully acknowledged. A.V.B., A.A.B., and H.O. are grateful to the DFG (Project 436 RUS/113/69/0-7) and RFBR Pprojects 09-03-91340a and 10-03-00320a) for financial support. K.H. thanks the Fonds zur Förderung der wissenschaftlichen Forschung (FWF), Vienna, for financial support of Project P 18176-N11. The authors are grateful to Mr. D. Müller at the University Karlsruhe for carrying out HRMS of the title compound.

**Supporting Information Available:** Molecular intensity curve for the GED experiment. Simulated spectra and parameters derived from the DNMR analysis. Total energies and relative energies of the minimum-energy pathway of **10** (Figure 7). M06-2X/pc-2 geometries of **10a** and **10e**. Tables of total and relative energies for **10a** and **10e**. Shielding constants and relative chemical shifts for the carbon nuclei of **10a** and **10e** at M06-2X/pc-2 geometries. Single-point PCM and IPCM energies of **10a** and **10e** in three different solvents compared with gas-phase energies. This material is available free of charge via the Internet at <http://pubs.acs.org>.

## References and Notes

- (1) Bodi, A.; Kvaran, Á.; Jonsdottir, S.; Antonsson, E.; Wallevik, S. Ó.; Arnason, I.; Belyakov, A. V.; Baskakov, A. A.; Hölbling, M.; Oberhammer, H. *Organometallics* **2007**, *26*, 6544.
- (2) Alabugin, I. V. *J. Org. Chem.* **2000**, *65*, 3910.
- (3) Alabugin, I. V.; Zeidan, T. A. *J. Am. Chem. Soc.* **2002**, *124*, 3175.
- (4) Cuevas, G.; Juaristi, E. *J. Am. Chem. Soc.* **2002**, *124*, 13088.
- (5) Leventis, N.; Hanna, S. B.; Sotiriou-Leventis, C. *J. Chem. Educ.* **1997**, *74*, 813.
- (6) Ribeiro, D. S.; Rittner, R. *J. Org. Chem.* **2003**, *68*, 6780.
- (7) Taddei, F.; Kleinpeter, E. *J. Mol. Struct. (Theochem)* **2004**, *683*, 29.
- (8) Taddei, F.; Kleinpeter, E. *J. Mol. Struct. (Theochem)* **2005**, *718*, 141.
- (9) Bushweller, C. H. Stereodynamics of Cyclohexane and Substituted Cyclohexanes. Substituent A Values. In *Conformational Behavior of Six-Membered Rings*; Juaristi, E., Ed.; VCH Publishers, Inc.: New York, 1995; pp 25.
- (10) Winstein, S.; Holness, N. J. *J. Am. Chem. Soc.* **1955**, *77*, 5562.
- (11) Wiberg, K. B.; Hammer, J. D.; Castejon, H.; Bailey, W. F.; DeLeon, E. L.; Jarret, R. M. *J. Org. Chem.* **1999**, *64*, 2085.
- (12) Weldon, A. J.; Vickerey, T. L.; Tschumper, G. S. *J. Phys. Chem. A* **2005**, *109*, 11073.
- (13) Shen, Q.; Hilderbrandt, R. L.; Mastryukov, V. S. *J. Mol. Struct.* **1979**, *54*, 121.
- (14) Favero, L. B.; Caminati, W.; Arnason, I.; Kvaran, A. *J. Mol. Spectrosc.* **2005**, *229*, 188.
- (15) Arnason, I.; Thorarinnsson, G. K.; Matern, E. *Z. Anorg. Allg. Chem.* **2000**, *626*, 853.
- (16) Arnason, I.; Kvaran, Á.; Bodi, A. *Int. J. Quantum Chem.* **2006**, *106*, 1975.
- (17) Arnason, I.; Kvaran, A.; Jonsdottir, S.; Gudnason, P. I.; Oberhammer, H. *J. Org. Chem.* **2002**, *67*, 3827.
- (18) Girichev, G. V.; Giricheva, N. I.; Bodi, A.; Gudnason, P. I.; Jonsdottir, S.; Kvaran, A.; Arnason, I.; Oberhammer, H. *Chem.—Eur. J.* **2007**, *13*, 1776.
- (19) Girichev, G. V.; Giricheva, N. I.; Bodi, A.; Gudnason, P. I.; Jonsdottir, S.; Kvaran, A.; Arnason, I.; Oberhammer, H. *Chem.—Eur. J.* **2009**, *15*, 8929.



- (20) Wallevik, S. Ó. Conformational behavior of substituted silacyclohexanes. M.Sc. Thesis, University of Iceland, 2008.
- (21) Bjornsson, R.; Arnason, I. *Phys. Chem. Chem. Phys.* **2009**, *11*, 8689.
- (22) Tsuboyama, A.; Murayama, A.; Konaka, S.; Kimura, M. *J. Mol. Struct.* **1984**, *118*, 351.
- (23) Andersen, P. *Acta Chem. Scand.* **1962**, *16*, 2337.
- (24) Carcenac, Y.; Diter, P.; Wakselman, C.; Tordeux, M. *New. J. Chem.* **2006**, *30*, 442.
- (25) Penman, K. G.; Kitching, W.; Adcock, W. *J. Org. Chem.* **1989**, *54*, 5390.
- (26) Shen, Q.; Rhodes, S.; Cochran, J. C. *Organometallics* **1992**, *11*, 485.
- (27) Cho, S. G.; Rim, O. K.; Kim, Y.-S. *J. Mol. Struct. (Theochem)* **1996**, *364*, 59.
- (28) Zheng, C.; Subramaniam, S.; Kalasinsky, V. F.; Durig, J. R. *J. Mol. Struct.* **2006**, *785*, 143.
- (29) Durig, J. R.; Ward, R. M.; Conrad, A. R.; Tubergen, M. J.; Giurgis, G. A.; Gounev, T. K. *J. Mol. Struct.* **2009**, *922*, 19.
- (30) *Inorganic Syntheses*; McGraw-Hill, Inc., 1968; Vol. XI.
- (31) West, R. *J. Am. Chem. Soc.* **1954**, *76*, 6012.
- (32) Ivanov, A. A.; Zasorin, E. *Z. Inst. Exp. Tech.* **1980**, *6*, 170.
- (33) Reich, H. J. WinDNMR: Dynamic NMR Spectra for Windows. *J. Chem. Educ. Software 3D2*.
- (34) Andersen, B.; Seip, H. M.; Strand, T. G.; Stolevik, R. *Acta Chem. Scand.* **1969**, *23*, 3224.
- (35) Gundersen, G.; Samdal, S.; Seip, H. M. *Least squares structural refinement program based on gas electron-diffraction data*; Department of Chemistry, University of Oslo: Oslo, 1981; Vol. I–III.
- (36) Ross, A. W.; Fink, M.; Hilderbrandt, R. L. *International Tables of Crystallography, C*; Kluwer Acad. Publ.: Dordrecht, 1992.
- (37) Sipachev, V. A. *J. Mol. Struct. (Theochem)* **1985**, *121*, 143.
- (38) Sipachev, V. A. *Vibrational effects in diffraction and microwave experiments: A start on the problem*; JAI Press: New York, 1999; Vol. 5.
- (39) Klaeboe, P. *Vib. Spectrosc.* **1995**, *9*, 3.
- (40) Frisch, M. J.; Trucks, G. W.; Schlegel, H. B.; Scuseria, G. E.; Robb, M. A.; Cheeseman, J. R.; J. A. Montgomery, J.; Vreven, T.; Kudin, K. N.; Burant, J. C.; Millam, J. M.; Iyengar, S. S.; Tomasi, J.; Barone, V.; Mennucci, B.; Cossi, M.; Scalmani, G.; Rega, N.; Petersson, G. A.; Nakatsuji, H.; Hada, M.; Ehara, M.; Toyota, K.; Fukuda, R.; Hasegawa, J.; Ishida, M.; Nakajima, T.; Honda, Y.; Kitao, O.; Nakai, H.; Klene, M.; Li, X.; Knox, J. E.; Hratchian, H. P.; Cross, J. B.; Bakken, V.; Adamo, C.; Jaramillo, J.; Gomperts, R.; Stratmann, R. E.; Yazyev, O.; Austin, A. J.; Cammi, R.; Pomelli, C.; Ochterski, J. W.; Ayala, P. Y.; Morokuma, K.; Voth, G. A.; Salvador, P.; Dannenberg, J. J.; Zakrzewski, V. G.; Dapprich, S.; Daniels, A. D.; Strain, M. C.; Farkas, O.; Malick, D. K.; Rabuck, A. D.; Raghavachari, K.; Foresman, J. B.; Ortiz, J. V.; Cui, Q.; Baboul, A. G.; Clifford, S.; Cioslowski, J.; Stefanov, B. B.; Liu, G.; Liashenko, A.; Piskorz, P.; Komaromi, I.; Martin, R. L.; Fox, D. J.; Keith, T.; Al-Laham, M. A.; Peng, C. Y.; Nanayakkara, A.; Challacombe, M.; Gill, P. M. W.; Johnson, B.; Chen, W.; Wong, M. W.; Gonzalez, C.; Pople, J. A. *Gaussian 03, Revision C.02*; Gaussian, Inc.: Wallingford CT, 2004.
- (41) Zhao, Y.; Truhlar, D. G. *Acc. Chem. Res.* **2008**, *41*, 157.
- (42) Zhao, Y.; Truhlar, D. G. *Theor. Chem. Acc.* **2008**, *120*, 215.
- (43) Jensen, F. *J. Chem. Phys.* **2001**, *115*, 9113.
- (44) Jensen, F.; Helgaker, T. *J. Chem. Phys.* **2004**, *121*, 3463.
- (45) Sinnokrot, M. O.; Sherrill, C. D. *J. Phys. Chem. A* **2004**, *108*, 10200.
- (46) Weldon, A. J.; Tschumper, G. S. *Int. J. Quantum Chem.* **2007**, *107*, 2261.
- (47) Dunning, T. H. *J. Chem. Phys.* **1989**, *90*, 1007.
- (48) Woon, D. E.; Dunning, T. H. *J. Chem. Phys.* **1993**, *98*, 1358.
- (49) Helgaker, T.; Klopper, W.; Koch, H.; Noga, J. *J. Chem. Phys.* **1997**, *106*, 9639.
- (50) Schwabe, T.; Grimme, S. *Phys. Chem. Chem. Phys.* **2007**, *9*, 3397.
- (51) Schwabe, T.; Grimme, S. *Acc. Chem. Res.* **2008**, *41*, 569.
- (52) Weigend, F.; Ahlrichs, R. *Phys. Chem. Chem. Phys.* **2005**, *7*, 3297.
- (53) Hamprecht, F. A.; Cohen, A.; Tozer, D. J.; Handy, N. C. *J. Chem. Phys.* **1998**, *109*, 6264.
- (54) Merrick, J. P.; Moran, D.; Radom, L. *J. Phys. Chem. A* **2007**, *111*, 11683.
- (55) Dos Santos, H. F.; Rocha, W. R.; De Almeida, W. B. *Chem. Phys.* **2002**, *280*, 31.
- (56) Franco, M. L.; Ferreira, D. E.; Dos Santos, H. F.; De Almeida, W. B. *J. Chem. Theory. Comput.* **2008**, *4*, 728.
- (57) Ayala, P. Y.; Schlegel, H. B. *J. Chem. Phys.* **1998**, *108*, 2314.
- (58) McClurg, R. B.; Flagan, R. C.; Goddard III, W. A. *J. Chem. Phys.* **1997**, *106*, 6675.
- (59) Pitzer, K. S.; Gwinn, W. D. *J. Chem. Phys.* **1942**, *10*, 428.
- (60) Truhlar, D. G. *J. Comput. Chem.* **1991**, *12*, 266.
- (61) Barone, V.; Cossi, M.; Tomasi, J. *J. Comput. Chem.* **1998**, *19*, 404.
- (62) Foresman, J. B.; Keith, T. A.; Wiberg, K. B.; Snoonian, J.; Frisch, M. J. *J. Phys. Chem.* **1996**, *100*, 16098.
- (63) Dichtfield, R. *Mol. Phys.* **1974**, *27*, 789.
- (64) Wolinski, K.; Hinton, J. F.; Pulay, P. *J. Am. Chem. Soc.* **1990**, *112*, 8251.
- (65) Adamo, C.; Barone, V. *Chem. Phys. Lett.* **1998**, *298*, 113.